HYBRID OPTIMIZATION FOR HIGH ASPECT RATIO WINGS WITH CONVOLUTIONAL NEURAL NETWORKS AND SQUIRREL OPTIMIZATION ALGORITHM

PENGFEI LI*

Abstract. An efficient hybrid optimization algorithm is introduced in this paper to optimize the lightweight design of high-aspect-ratio wings, tackling the complexities associated with the mixed optimization design of layout and size variables within these wing structures. A hybrid binary unified coding description facilitates the optimization process for layout and size variables. The study influences one-dimensional convolutional neural networks to establish an aeroelastic surrogate model, primarily chosen for their exceptional performance in handling multi-parameter aeroelastic regression problems. Additionally, the squirrel optimization algorithm is chosen over the genetic algorithm for the mixed optimization problem, leading to notable savings in computational costs. The research demonstrates that the proposed hybrid optimization method, integrating the one-dimensional convolutional neural network and the squirrel optimization algorithm, offers superior performance in optimizing high aspect ratio wings. Specifically, it results in a reduction of 4.1% in the weight of the wing structure. Moreover, the study highlights the necessity of this hybrid approach due to the observed coupling between the layout variables of the wing ribs and the size variables of the wing beams.

Key words: High aspect ratio wings; Structural optimization design; Hybrid optimization; Convolutional neural network; Squirrel optimization algorithm

1. Introduction. Rotating machinery is critical in contemporary industrial production, constituting approximately 80

The evolution of fault diagnosis technology has progressed with mechanical advancements, unfolding across four distinct stages: During the 19th century, mechanical equipment possessed relative simplicity, warranting post-maintenance measures. Subsequently, from the early 20th century to the 1950s, the increasing complexity of machinery began to disrupt the smooth flow of production and daily life, prompting the adoption of regular maintenance as a diagnostic approach. The 1960s and 1970s witnessed a turning point with computer technology's maturation, leading to more sophisticated diagnostic methodologies that involved observing data patterns during machine operations and implementing targeted maintenance strategies [2].

The trajectory of fault diagnosis technology, foreseeing its alignment with the progression of intelligent decision-making capabilities in industrial big data, is grounded in the theoretical principles of data science. The Convolutional Neural Network (CNN) is a prominent model within deep neural networks, drawing significant attention since its initial exploration in the 1980s. Inspired by the biological visual perception mechanism, it boasts a remarkable capacity for representational learning. Notably, CNN retains its efficacy in challenging scenarios characterized by complex environmental information, ambiguous background knowledge, obscure inference rules, and samples with substantial impairments [3].

The rise of data-driven methodologies has recently witnessed widespread adoption across various domains. Its application aims to decipher the operational state of systems through data analysis, facilitating decision-making and control of equipment and production processes. Consequently, it has emerged as the prevailing technology for fault diagnosis. This approach relies on diverse datasets, delving into the intrinsic data patterns via machine learning and statistical analysis techniques, thus enabling the construction of fault diagnosis models. The author's study explores data-driven fault diagnosis methods, which can be categorized into three key stages: data collection, feature extraction, and fault classification [4].

The advancement of industrial big data is propelling the adoption of data-driven fault diagnosis methods, integrating an ever-growing range of data sources. Commonly employed data types encompass current, acoustic emission (AE), and vibration data. Particularly, fault diagnosis techniques reliant on vibration data have

* Zhengzhou Railway Vocational and Technical College, Zhengzhou, 451460, China (`pengfeili69@163.com`).

garnered substantial traction within the industrial sphere. Vibration data derived from machinery can effectively capture diverse indicators related to multiple components and structures, including gear meshing frequency, bearings, structural resonance, and electrical anomalies [5].

The direct installation of sensors on the casing of the monitored component presents a distinct advantage, as it minimizes the potential interference of received signals. Since the inception of the first solar-powered drone, Sunrise, more than 40 years ago, the development of High Altitude Long Endurance (HALE) solar-powered drones has been ongoing. To fulfil the demanding prerequisites of high lift-to-drag ratios and lightweight designs, the wings of these high-altitude, long-endurance aircraft are predominantly engineered with high aspect ratios and notable flexibility. This particular design paradigm, however, exhibits a heightened sensitivity to the aircraft's overall weight. Therefore, the primary goal of the structural optimization design for solar-powered unmanned aerial vehicles remains the achievement of lightweight design while ensuring the fulfilment of structural strength and stiffness requirements [6].

Two distinct strategies have emerged in addressing such complex multi-parameter structural optimization problems: the variable-by-variable and comprehensive optimization methods. While the former approach over-looks the interdependencies between multiple variables, the latter involves the mixed optimization of multiple variables, thereby considering the intricate relationships among various parameters to obtain an ultimate global optimal solution. However, this holistic approach is challenging due to its high computational complexity [7].

The authors proposed a multi-objective optimization approach for three-dimensional truss tower structures, employing enhanced Pareto evolutionary algorithms, population-based incremental learning algorithms, and archived simulated annealing algorithms to overcome the general challenges. Simultaneously, a hybrid optimization strategy for the layout and topology of reinforcing ribs in plate and shell structures using the Solid Isotropic Material with Penalization (SIMP) model and the basic structure method successfully verified the reliability of this method [8].

The structural design of solar-powered drone wings and the intricate aeroelastic characteristics stemming from high-flexibility wings under aerodynamic loads underscore the critical importance of establishing a highly reliable aeroelastic model. As computational technology has advanced, numerical calculations, notably Computational Fluid Dynamics/Computational Structural Dynamics (CFD/CSD) fluid-structure coupling technology, have assumed a pivotal role in aircraft optimization design. Traditional surrogate models, including the Polynomial Response Surface (PRS) model and the Kriging model, have been complemented by the emerging prominence of deep learning-based surrogate models, particularly adept at handling high-dimensional nonlinear problems [9].

The design of the hybrid optimization model encompasses a strategic fusion of multiple methodologies to tackle the intricacies of optimizing high aspect ratio wing structures. A pivotal element within this framework is implementing a unified coding scheme meticulously tailored to encapsulate layout and size variables. This coding methodology ensures a coherent representation of the intricate structural parameters, forming the cornerstone of the optimization process.

2. Analytical Methods. A suitable one-dimensional convolutional neural network structure is designed using a specific optimization algorithm and loss function. Using CFD/CSD technology to calculate the aeroelastic data of solar unmanned aerial vehicle wings with a high aspect ratio and using reasonable coding methods to encode the structural and aeroelastic data according to the characteristics of the wings with high aspect ratio, the aeroelastic surrogate model is obtained by training the one-dimensional convolutional neural network model. Based on the surrogate model, the squirrel optimization algorithm is used for optimization [10].

2.1. Aeroelastic surrogate model based on one-dimensional convolutional neural network.
(1) A one-dimensional convolutional neural network model The CNN functioning as a multilevel feedforward neural network is structured with distinct layers, including an input layer, a convolutional layer, an activation layer, a pooling layer, a fully connected layer, and an output layer. Its prevalence in computer vision tasks stems from its capability to extract features from localized input blocks and subsequently modularize them, optimizing data utilization. In one-dimensional sequence recognition, the distinct attributes of one-dimensional convolutional neural networks, such as pattern learning, translation invariance, and spatial hierarchy, can be effectively leveraged for multi-parameter regression analysis [11].

In deep learning, the optimization algorithm fine-tuns weight values to identify the optimal parameter combination that minimizes the loss function value. Commonly employed optimization algorithms for CNN include Stochastic Gradient Descent (SGD), SGD with Momentum, RMSProp, and Adam [12]. The expression for gradient weight is given by

$$g_t = \frac{1}{n} \nabla(\theta_{t-1}) \sum_{i=1}^{n} L(f(x_i, \theta_{t-1}), y_i) \tag{2.1}$$

In Equation 2.1, g_t is the weight gradient, n is the number of small batch samples, θ is the weight, l is the time step, $f(x, \theta)$ is the forward inference result of the convolutional neural network. Y is the real label, $L(\hat{y}, y)$ is the loss function, the author trains the data set by using different loss functions and selects the loss function most suitable for determining the Mean Squared Error (MSE).

(2) Structural parameter coding

For regression analysis, the convolutional neural network necessitates a training dataset. The training dataset comprises structural parameters and aeroelastic result data within the aeroelastic surrogate model. The structural data is encoded using suitable encoding methods, while the dimensional parameters are binary. Ultimately, the two are combined into a sequence, taking the following form:

$$T_{1,1}, T_{1,2}, ..., T_{2,1}, ..., T_{n,m} | S_{1,1}, S_{1,2}, ..., S_{2,1}, ..., S_{n,m} \tag{2.2}$$

where

$$T_{i,j}\epsilon\{0,1\}, S_{i,j} = \{a_{i,j,1}, a_{i,j,2}, ..., a_{i,j,l}\}, a_{i,j,k}\epsilon\{0,1\} \tag{2.3}$$

In the Formula, $T_{i,j}$ represents whether the ith structural member exists at position j, θ indicates nonexistence, 1 indicates existence; N represents the total number of structures, and m represents the total number of structural distribution positions; $S_{i,j}$ represents the size of the ith-type structural component at position j, composed of binary code $a_{i,j,k}$; L represents the binary encoding tension.

(3) Aeroelastic surrogate model

The acquisition of sample data involves aeroelastic simulation calculations, with subsequent binary encoding of the structure. This data is then inputted into the one-dimensional convolutional neural network for training, resulting in the generation of the surrogate model, as illustrated in Figure 2.1. The aeroelastic simulation employs CFD/CSD bidirectional coupling technology, wherein the fluid domain and structure are solved independently, and data in the time domain are staggered to achieve progressive advancements, ultimately deriving the aeroelastic data of the coupled system. During the training of sample data using one-dimensional convolutional neural networks, the elastic axis displacement of the wing tip is designated as the prediction target. The average absolute error value (MAE) serves as the evaluation metric, prompting continuous adjustments to the network structure and ensuring improved prediction accuracy of the surrogate model [13,14].

2.2. Squirrel Optimization Algorithm. The Squirrel Search Algorithm (SSA) is an intelligent swarm-based optimization algorithm inspired by squirrels' foraging behaviour and aerodynamics for its rapid convergence and robust optimization capabilities [15,16]. The algorithm operates according to the following process:

(1) Random initialization

$$FS = \begin{bmatrix} FS_{1,1} FS_{1,2}...FS_{1,d} \\ FS_{2,1} FS_{2,2}...FS_{2,d} \\ ... \\ FS_{n,1} FS_{n,2}...FS_{n,d} \end{bmatrix} \tag{2.4}$$

The Equation $FS_{i,j}$ represents the value of the ith squirrel in the jth dimension, which can be evenly distributed using Equation 2.5.

$$FS_i = FS_L + U(0,1) \times (FS_U - FS_L) \tag{2.5}$$
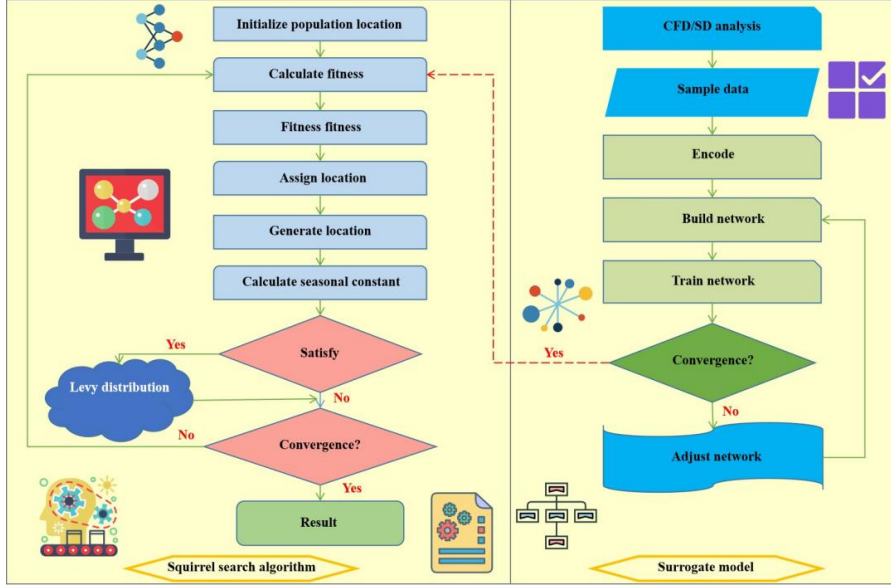
Fig. 2.1: Proposed Hybrid Optimization for High Aspect Ratio Wings with CNN and SSA

In Equation 2.5, FS_L and FS_U are the lower and upper bounds of the position of the ith squirrel, and U $(0,1)$ is a uniformly distributed random number within the range of $[0,1]$[17].

(2) Fitness evaluation

Applying a user-defined fitness function involves computing the positional fitness for each squirrel. Subsequently, the fitness values are arranged in ascending order. Squirrels with the minimum fitness are allocated to the hickory tree, while the subsequent three squirrels reside on oak trees, leaving the remaining to settle on ordinary trees. The foraging behaviour of squirrels is also influenced by predators, with a probability of P_{dp} $=0.1$.

(3) Generate new location

Squirrels encounter three scenarios during their active foraging process: The initial situation involves transitioning from an oak tree to a hickory tree:

$$FS_{at}^{t-1} = \begin{cases} FS_{at}^t + d_g \times G_c \times (FS_{ht}^t - FS_{at}^t), R_l \geqslant P_{dp} \\ Random, location, otherwise \end{cases} \tag{2.6}$$

In the Formula, d_g is the random gliding distance, R_1 is a random number of $[0,1]$, FSat is the position of the squirrel on the oak tree, FS_{ht} is the position where the squirrel reaches the hickory tree, and G_c is the sliding coefficient. To balance global and local search, G_c is generally taken as 1.9. In the second case, flying from a regular tree to an oak tree:

$$FS_{nt}^{t+1} = \begin{cases} FS_{nt}^t + d_g \times G_c \times (FS_{at}^t - FS_{nt}^t), R_2 \geqslant P_{dp} \\ Random, location, otherwise \end{cases} \tag{2.7}$$

In Equation 2.7, R_2 is a random number in $[0,1]$, and FS_{nt} is the squirrel's position on a regular tree. The third scenario: Flying from a regular tree to a hickory tree:

$$FS_{nt}^{t+1} = \begin{cases} FS_{nt}^t + d_g \times G_c \times (FS_{ht}^t - FS_{nt}^t), R_3 \geqslant P_{dp} \\ Random, location, otherwise \end{cases} \tag{2.8}$$

where, R_3 is a random number in $[0,1]$.

(4) Seasonal variation conditions

Seasonal monitoring conditions are incorporated into SSA to prevent the algorithm from becoming entangled in local optimal solutions. When these seasonal conditions are met, Levy Distribution introduces random positional changes for squirrels on ordinary trees [18].

2.3. Multi-parameter mixed optimization mathematical model for wing structure. According to the proposed structural coding method, the mathematical model of hybrid optimization can be expressed as:

$$
\begin{aligned}
& find, T, S \\
& min, m(T, S) \\
& s.t, g_i \leqslant 0. i = 1, ..., n \\
& T_{i,j} \epsilon \{0, 1\}. i = 1, ..., n. j = 1, ..., m \\
& S_i \epsilon [LB_i, UB_i]. i = 1, ..., n
\end{aligned}
\tag{2.9}
$$

The Formula incorporates T as the layout variable for the structural component, assuming values of 0 or 1. S represents the dimensional variable of the structural component, whereas M(T, S) signifies the structural mass. gi denotes the constraint conditions of the structure, while LB and UB denote the lower and upper bounds of structural size variables. The overall optimization algorithm process is visualized in Figure 2.1. The initial step involves acquiring sample data through aeroelastic simulation calculation, encompassing structural parameters alongside their corresponding wingtip elastic axis displacement. Subsequently, the structure undergoes binary encoding [19].

Integrating the squirrel optimization algorithm and the surrogate model, derived from training in generating a one-dimensional convolutional neural network, initiates the hybrid optimization process. Initially, the squirrel dimension is determined based on the number of variables. Subsequently, a decimal description is employed for initialization, and the corresponding squirrel position is coded, as demonstrated in Equation 2.2. The fitness value is computed using the surrogate model, enabling the sorting and allocating of squirrel positions across various tree types according to their respective fitness values.

Subsequent reallocation of squirrel positions is facilitated using Equations 2.6 to 2.8. The decision to redistribute squirrel positions utilizing the Levi distribution is contingent upon satisfying seasonal conditions. This iterative process continues until the optimization result is achieved [20].

3. Example analysis of wing structure optimization design. The ribs and beams are the primary load-bearing components of solar-powered drone wings with high aspect ratios. The layout and size parameters associated with these ribs and beams are crucial variables dictating structural performance. The wing structure parameters are derived from relevant literature in the author's case study. Based on the wing model, variations are introduced in the distribution of wing ribs and the diameter of wing beams. Select models with distinct parameters are chosen as samples for aeroelastic numerical analysis. The selection criterion for these samples ensures that each parameter encompasses diverse values, albeit not covering all potential values.

3.1. Numerical and Optimization Models for Wings. The wing structure is characterized by a flat and straight design, featuring an Eppler387 airfoil, a chord length of 0.41m, and a span length of 2.5m. The materials utilized adhere to isotropic models. The composite material constituting the wing rib and wing beam boasts an $1800 kg/m^3$ density, a Poisson's ratio of 0.307, and an elastic modulus of 100GPa. Conversely, areas apart from the wing ribs and wing beams are filled with foam materials, showcasing a density of $20 kg/m^3$, a Poisson's ratio of 0.08, and an elastic modulus of 5.4MPa. The wing structure model comprises 11 evenly distributed wing ribs, each with a thickness of 2mm. Considering the dimensions of the solar panel, a maximum of 21 wing ribs can be uniformly distributed across all feasible positions on the structure. Regarding the wing profile shape, the inner diameters of the three wing beams are 8mm, 22mm, and 14mm, while the corresponding outer diameters are 10mm, 26mm, and 16mm, respectively. The variables subject to the author's optimization efforts are the distribution of wing ribs across 21 positions and the inner diameter of the three wing beams.

During the aeroelastic numerical analysis process, special attention is given to maintaining the grid height of the fluid domain grid within the first layer of the wing boundary layer at $y+ \approx 1$. This meticulous approach

Table 3.1: Parameters of convolutional neural networks

Layer	Type	Neuron	Activation
1	Input	32	-
2	Convolution	64	Relu
3	Max pooling	-	-
4	Convolution	128	Relu
5	Global average pooling	-	-
6	Dense	16	-
7	Output	1	-

ensures that the total number of grids is 3 million. Employing a standard $k - \varepsilon$ A turbulence model, the analysis considers an incoming flow velocity of $15m/s$ and a wing angle of attack $5°$. The solid domain grid is set at 500,000, with a fixed constraint at one wing beam's end. The original model's calculated elastic axis displacement of the wing tip measures 143.64mm, serving as a critical structural constraint condition.

3.2. Prediction accuracy verification of surrogate model. Utilizing the Adam algorithm, the author constructs a one-dimensional convolutional neural network to establish a hybrid optimization surrogate model. The neural network's architecture is detailed in Table 3.1.

The sample dataset comprises 180 groups, segregated into three groups using K-fold cross-validation. The AdaGrad, RMSProp, and Adam algorithms are applied to validate both the one-dimensional convolutional neural network and the fully connected network. The fully connected network comprises three hidden layers, with a network structure and the number of neurons mirroring those of the one-dimensional convolutional neural network. The evaluation metric employed is the Mean Absolute Error (MAE) value. The outcomes following 10,000 training iterations are illustrated in Figure 3.1, where Dense denotes the fully connected network and Convnet represents the one-dimensional convolutional network.

Figure 3.1 demonstrates the superior performance of the one-dimensional convolutional neural network optimized by the Adam algorithm. After 500 training steps, the MAE stabilizes without displaying signs of "overfitting." Post-convergence, the MAE mean settles around 0.8. Relative to the sample data featuring a displacement mean of 150mm, the relative error approximates 0.5%. This outcome underscores the efficacy of the surrogate model in addressing multi-parameter aeroelastic regression issues [21].

3.3. Feasibility verification of hybrid optimization algorithm. The preceding analysis demonstrates the viability of establishing an aeroelastic surrogate model using the one-dimensional convolutional neural network optimized via the Adam algorithm. Building upon this surrogate model, this section validates the practicality of the hybrid layout and size optimization algorithm within the wing structure optimization design process. To assess its efficacy, the results of the squirrel optimization algorithm were juxtaposed with those of the genetic algorithm, maintaining uniformity in key parameters such as the probability of random population changes.

The optimization capabilities are compared for the two algorithms with smaller population sizes. Fifty calculations were executed at populations of 50 and 100, respectively. The changes in average wingtip displacement and structural mass were recorded across iteration steps, illustrated in Figure 3.2 (with GA_50 and GA_100 representing genetic algorithms with populations of 50 and 100, respectively, and SSA_50 and SSA_100 representing squirrel optimization algorithms with populations of 50 and 100, respectively). Furthermore, the time taken for 1000 iterations of the two algorithms on the Inteli7-3770 processor was documented, as presented in Table 3.2 (where GA and SSA denote genetic algorithms and squirrel optimization algorithms, respectively) [22].

The observations from Figure 3.2 underscore that throughout the optimization procedure, the squirrel optimization algorithm outperforms the genetic algorithm in locating optimal values, showcasing superior stability in terms of wingtip displacement and structural mass. Examination of Table 3.2 reveals that the squirrel optimization algorithm demonstrates a more efficient time utilization when addressing this specific mixed opti-
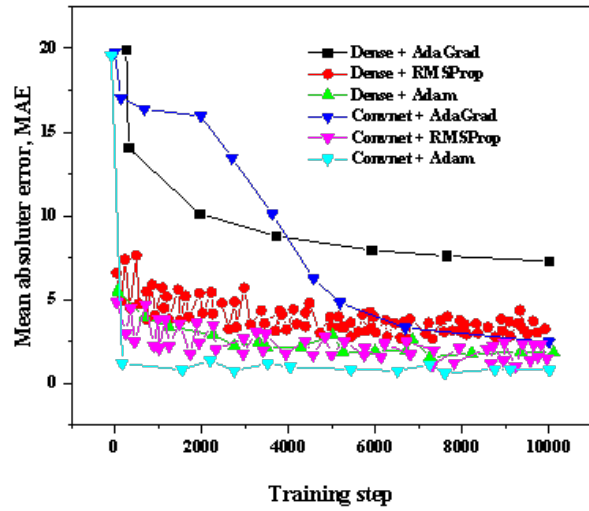
Fig. 3.1: Average Absolute Error Variation of Different Neural Networks
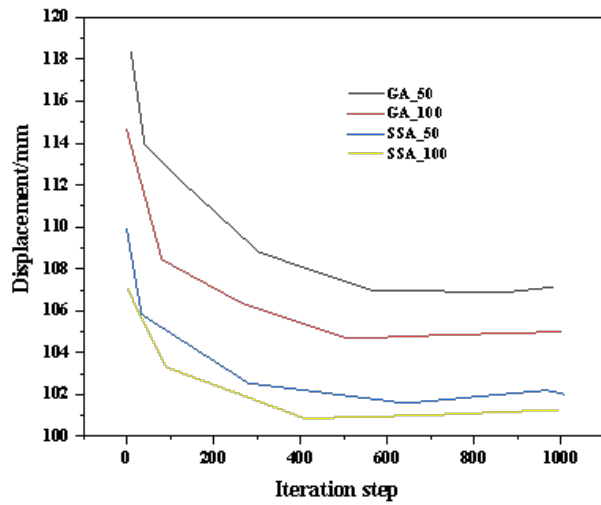
Fig. 3.2: Iteration History of Wing Tip Displacement and Structural Mass

mization problem. Notably, the time consumption is reduced by 45.51% with a population size of 50 and by 35.80% when the population is 100.

Employing the squirrel optimization algorithm with a population size of 100, the individual layout variables of wing ribs and the mixed optimization problem of wing rib layout variables and wing beam size variables were optimized, resulting in an optimized wing structure with a refined wing rib layout and a hybrid optimization of wing rib layout and wing beam size.

The optimized wing layout features five fewer ribs than the original structure, resulting in a weight of

Table 3.2: Time consumption of two optimization algorithms

Algorithm	Population	Time(s)
Genetic Algorithm(GA)	50	72.90
	100	83.81
Squirrel Search Algorithm(SSA)	50	40.09
	100	53.81

1.6588kg, marking a 3.1% reduction compared to the original design. As depicted in Figure 3.2, the mixed optimization of layout and size variables results in the wing comprising five wing ribs. Additionally, the inner diameter of the wing beams now varies from front to back, measuring 9mm, 21mm, and 15mm, respectively.

The comparison above highlights the superior performance of the aeroelastic surrogate model, established through the one-dimensional convolutional neural network, effectively handling mixed regression problems related to structure distribution and size. Comparatively, when addressing mixed optimization problems, the squirrel optimization algorithm outperforms the genetic algorithm, yielding better solutions at reduced computational costs.

4. Conclusion. The author introduces an effective hybrid optimization algorithm to target the mixed optimization design challenge inherent in the layout and size of high aspect ratio wings. Leveraging the unified coding of multiple variables, the study implements a one-dimensional convolutional neural network to establish an aeroelastic surrogate model. This is complemented by a solution workflow structured around the squirrel optimization algorithm for comprehensive search and optimization. The study highlights the efficacy of the proposed hybrid layout and size optimization method for achieving lightweight design objectives in high aspect ratio wings. Based on comprehensive CFD/CSD aeroelastic calculations and uniform coding of diverse structural variables, the surrogate model demonstrates the significant capabilities of the one-dimensional convolutional neural network. Applying the squirrel optimization algorithm effectively reduces computational costs by 35% to 45% compared to the genetic algorithm. Furthermore, the hybrid optimized structure showcases a notable 4.1

REFERENCES

[1] Wang, Z. , Lyu, Z. , Duan, D. , & Li, J. . (2021). A novel system identification algorithm for quad tilt-rotor based on neural network with foraging strategy: Proceedings of the Institution of Mechanical Engineers, Part G: Journal of Aerospace Engineering, 235(11), 1474-1487.
[2] Kan, Z. , & Liu, X. . (2021). The study on void fraction prediction of gas-liquid two phase flow based on convolutional neural network. Journal of Physics: Conference Series, 2121(1), 012029.
[3] Liu, C. , He, J. , Wang, P. , Xing, D. , Li, J. , & Liu, Y. , et al. (2023). Characteristic extraction of soliton dynamics based on convolutional autoencoder neural network. Chinese Optics Letters, 21(3), 031901.
[4] Hu, Z. X., Wang, Y., Ge, M. F., & Liu, J. (2019). Data-driven fault diagnosis method based on compressed sensing and improved multiscale network. IEEE Transactions on Industrial Electronics, 67(4), 3216-3225.
[5] Yan, J., Meng, Y., Lu, L., & Li, L. (2017). Industrial big data in an industry 4.0 environment: Challenges, schemes, and applications for predictive maintenance. IEEE access, 5, 23484-23491.
[6] Wang, X., Yang, Y., Wu, D., Zhang, Z., & Ma, X. (2020). Mission-oriented 3D path planning for high-altitude long-endurance solar-powered UAVs with optimal energy management. IEEE Access, 8, 227629-227641.
[7] Liao, T., Socha, K., de Oca, M. A. M., Stützle, T., & Dorigo, M. (2013). Ant colony optimization for mixed-variable optimization problems. IEEE Transactions on evolutionary computation, 18(4), 503-518.
[8] Deb, K. (2003). Multi-objective evolutionary algorithms: Introducing bias among Pareto-optimal solutions. In Advances in evolutionary computing: theory and applications (pp. 263-292). Berlin, Heidelberg: Springer Berlin Heidelberg.
[9] Huang, C., Huang, J., Song, X., Zheng, G., & Yang, G. (2021). Three dimensional aeroelastic analyses considering free-play nonlinearity using computational fluid dynamics/computational structural dynamics coupling. Journal of Sound and Vibration, 494, 115896.
[10] Ahmad, S. N. , & Prakash, O. . (2021). Optimization of ground heat exchanger of the ground source heat pump system based on exergetic analysis using taguchi technique:. Proceedings of the Institution of Mechanical Engineers, Part C: Journal of Mechanical Engineering Science, 235(21), 5892-5901.
[11] Yang, Y., Nie, Z., Huang, S., Lin, P., & Wu, J. (2019). Multilevel features convolutional neural network for multifocus image fusion. IEEE Transactions on Computational Imaging, 5(2), 262-273.

[12] Newton, D., Yousefian, F., & Pasupathy, R. (2018). Stochastic gradient descent: Recent trends. Recent advances in optimization and modeling of contemporary problems, 193-220.

[13] Dolezel, P. , Holik, F. , Merta, J. , & Stursa, D. . (2021). Optimization of a depiction procedure for an artificial intelligence-based network protection system using a genetic algorithm. Applied Sciences, 11(5), 2012.

[14] Li, Z. , Wang, Y. , & Ma, J. . (2021). Fault diagnosis of motor bearings based on a convolutional long short-term memory network of bayesian optimization. IEEE Access, PP(99), 1-1.

[15] Li, C. , Yin, C. , & Xu, X. . (2021). Hybrid optimization assisted deep convolutional neural network for hardening prediction in steel. Journal of King Saud University - Science, 33(6), 101453.

[16] Alshaikhli, O. A. , & Al-Araji, A. . (2021). Path planning and control strategy design for mobile robot based on hybrid swarm optimization algorithm. International Journal of Intelligent Engineering and Systems, 14(3), 2021.

[17] He, Y. . (2021). Design and implementation of convolutional neural network accelerator based on riscv. Journal of Physics: Conference Series, 1871(1), 012073 (5pp).

[18] Fares, D., Fathi, M., Shams, I., & Mekhilef, S. (2021). A novel global MPPT technique based on squirrel search algorithm for PV module under partial shading conditions. Energy Conversion and Management, 230, 113773.

[19] Tanveer, A., & Ahmad, S. M. (2023). Mathematical Modelling and Fluidic Thrust Vectoring Control of a Delta Wing UAV. Aerospace, 10(6), 563.

[20] Zhao, X., Tang, Z., Cao, F., Zhu, C., & Periaux, J. (2022). An Efficient Hybrid Evolutionary Optimization Method Coupling Cultural Algorithm with Genetic Algorithms and Its Application to Aerodynamic Shape Design. Applied Sciences, 12(7), 3482.

[21] Li, W., Gao, X., & Liu, H. (2021). Efficient prediction of transonic flutter boundaries for varying Mach number and angle of attack via LSTM network. Aerospace Science and Technology, 110, 106451.

[22] Vidushi, Agarwal, M. , Rajak, A. , & Shrivastava, A. K. . (2021). Assessment of optimizers impact on image recognition with convolutional neural network to adversarial datasets. Journal of Physics: Conference Series, 1998(1), 012008.